Hydrothermal leaching behavior of complex polymetallic secondary sulfide concentrate enhanced by ultrasonic

Q.F. Liu, Y.L. Liao*, J.L. Li, M. Wu

Qingfeng Liu (ORCID: 0009-0008-3046-0418), Yalong Liao*(ORCID: 0000-0001-8179-2342), Jialei Li (ORCID: 0009-0006-5342-5469), Min Wu (ORCID: 0009-0004-4527-8003)
(Faculty of Metallurgical and Energy Engineering, Kunming University of Science and Technology, Kunming 650093, China)

Corresponding author: Yalong Liao, Xuefu Road 253, Faculty of metallurgical and energy engineering, Kunming university of science and technology, Yunnan Kunming 650093, China. *E-mail:* liaoyl@kust.edu.cn.

(Received 18 June 2024; Accepted 21 March 2025)

Abstract: Complex polymetallic secondary sulfide concentrate (CPSSC) is difficult to efficiently be utilized because of its special mineral phase structure and high content of lead and iron. A novelty process proposed in this study, hydrothermal leaching without acid (water as lixiviate) enhanced by ultrasonic, can achieve eco-friendly and selective separation of copper from CPSSC, inhibiting production of hazardous material plumboferrite contained in leached residue. The influence of controlling parameters on the leaching efficiency and the mineral phase composition and structure of the obtained leached residue are studied. The obtained results show that, without sulfuric acid, the leaching efficiency of copper is the best under the conditions of temperature 180 ℃, oxygen partial pressure 1.0 MPa, stirring speed 600 r/min, ultrasonic power 360 W, liquid-solid ratio 10:1 and mass ratio of lignosulfonate to raw material 0.2%. Under the above optimal conditions, the leaching efficiency of copper and iron reached 99.12% and 19.46%, respectively. Ultrasonic enhancement increases the copper leaching efficiency by 10.02%, and promotes the leaching efficiency of iron decreases by 5.20%. The leaching process conforms the unreacted contraction core model under mixed control, the activation energy is 71.76 kJ/mol, and the macroscopic kinetic equation related to stirring rate, oxygen partial pressure and ultrasonic

power is $1-(1-X)^{1/3} -1/3\ln(1-X) = 40.457P_{O_2}^{0.771}r^{0.903}P^{0.431}e^{(-8630.19/T)}t$。

Kew words：chalcopyrite；process enhancement；hydrothermal leaching；kinetics

1. Introduction

Chalcopyrite ($CuFeS_2$) is the most abundant and widely distributed copper bearing mineral, but with the continuous mining of copper ore, not only the grade of copper in original chalcopyrite ore has declined year by year, but also it co-exists with iron, lead, arsenic and other elements. Moreover the flotation properties of copper and lead are similar, it is still difficult to obtain the concentrates required by pyrometallurgical process through beneficiation operations from the original chalcopyrite ore. This resulted in the existence of a large number of complex polymetallic secondary sulfide concentrate (CPSSC). When traditional pyrometallurgical method is used to treat the CPSSC, on the one hand the recovery of copper is low, and on the other hand a large amount of lead scum and hazardous gases will be produced in the process. Although some copper and lead contained in the lead scum, they are difficult to be recycled. The produced harmful gases, such as CO, NxOy, and SO_2, pose a potential threat to the environment and human body. In comparison, hydrometallurgy is more economical and environmentally friendly to extract valuable metals like copper from CPSSC. Hydrometallurgical leaching of CPSSC shows great potential in terms of addressing the environmental impacts and decreasing the treating cost [1]. However, due to the unique mineral phase structure of chalcopyrite the main mineral phase existing in CPSSC [2], passivating layers which consist of bimetallic sulfides, polysulfides, elemental sulfur and jarosite can be formed on the surface of chalcopyrite particle during leaching , resulting in low leaching efficiency of valuable metals [3-4]. Thus restricting the promotion and development of this environmentally friendly method for dispose CPSSC. Therefore, it is urgent to strengthen the leaching process of CPSSC and improve the leaching efficiency of copper for utilizing this kind of resource.

In recent years, the methods to enhance chalcopyrite leaching include pretreatment activation and

strengthening during leaching process are researched and reported. Pretreatment activation includes mechanical activation [5-7], thermal activation [8] and microwave activation [9-10], which can improve the reactivity of chalcopyrite in leaching. The strengthening methodology in the leaching process includes adding additives such as pyrite [11-12], Ag ion [13-14] and activated carbon to strengthen the leaching [15-16], and external field strengthening by ultrasonic field, microwave field [17-18] and pressure field [19].

However, the leaching strengthened by pressure field could achieve more than 98% leaching efficiency of Cu from low-grade polymetallic complex chalcopyrite ore, the conditions needed in the leaching process are harsh which with a high temperature (200 ℃) and high O_2 partial pressure (1.2 MPa) [20]. Therefore, it is necessary to study pressure enhanced leaching under friendly conditions. Studies showed that the leaching efficiency of copper from chalcopyrite would be significantly improved when the leaching system was in the ultrasonic field [21-24]. Wang's investigation demonstrated that the leaching efficiency of copper increased to 57.5% from 50.4% in an oxygenated acidic ferric solution while ultrasonic enhancement was performed in leaching process of concentrated chalcopyrite containing 18.2% Cu [25]. Yoon [26] used $FeCl_3$ solution as lixiviant to dispose chalcopyrite ($CuFeS_2$) containing 41.5% Cu, and under the enhanced action of ultrasound, the leaching efficiency of copper increased to 87% from 77%. When the ultrasonic field was induced in the leaching system, ultrasonic cavitation effect would be produced, resulting high temperature and high pressure and luminous discharge phenomena in some micro-area in the leaching solution. By creating such an extreme environment, ultrasound could improve the efficiency of material transfer and phase interface renewal, and promoted the break of intermolecular bonding bonds to activate molecules, thus playing a significant role in promoting the leaching process [27]. The research employed by Wang [28] showed that the leaching efficiency of copper increased to 6.2% from 5.4% while leaching process of low grade of primary copper sulfide ore containing 0.49% Cu was enhanced with ultrasonic in comparison to that of without enhancement. However, the leaching systems involved in these studies are mainly high-valent iron ion systems with strong oxidation, or in

strong acidity medium, the medium without acid for hydrothermal leaching and the kinetics of leaching methodology enhanced with ultrasonic were rarely involved, especially not involved in oxygen pressurized system. Moreover, the raw materials used in these studies were concentrated chalcopyrite or primary sulfide copper ore, not involved in refractory ore likes CPSSC, and even though with concentrated chalcopyrite the obtained leaching efficiency of copper was not ideal.

From the above studies, it can be seen that both pressure field and ultrasonic strengthening can improve the leaching efficiency of copper from chalcopyrite, but there is few research on the combination of ultrasonic and pressure field to strengthen leaching copper from CPPSC. In this paper, a novelty process for eco-friendly utilizing CPSSC by joint enhanced methods with pressure field and ultrasonic filed was proposed. The effects of reaction temperature, initial acidity, oxygen partial pressure, stirring speed, ultrasonic power and liquid solid ratio on the leaching of CPSSC were studied, and the kinetics of ultrasonic enhanced copper leaching without acid (water as leaching agent) from CPSSC was studied.

2. Experimental

2.1.Materials and chemical agents

In the present work, CPSSC produced in beneficiation operations was friendly supplied by a concentrator of a mining company in Yunnan Province, China. Firstly, it was crushed by a ball mill (XMQ240×90, Jiangxi Victor International mining equipment Co., LTD, China) and screened with Standard Taylor sieve , and raw materials with particle size of -45 μm used to experiment were obtained. The content of chemical elements in the raw materials was determined by inductively coupled plasma emission spectrometry (ICP-AES) while the sample were dissolved with a mixture of hydrochloric, nitric and perchloric acids. The specific results were shown in table 1 which showed that besides the copper content in the raw material was only 11.10%, far lower than that

the required content of copper concentrate (Cu >18%) for disposing by traditional pyrometallurgical methodology, the content of iron and lead are high. Obviously, the raw material used in the present work was a typical low-grade polymetallic complex copper sulfide secondary concentrate.

Table 1 Chemical elemental analysis of raw materials

Cu	Fe	Pb	Zn	S	SiO_2	CaO	Al_2O_3	MgO	Others (CO_3^{2-}, SiO_3^{2-})
11.10	28.10	8.88	2.97	34.95	8.86	1.68	0.50	1.63	1.33

X-ray diffractometer (XRD, X 'Pert Pro MPD) was used to analyze the mineral phase composition of the raw material, and the obtained results were shown in figure 1. Fig. 1 shows that the mineral phases contained in CPSSC include chalcopyrite ($CuFeS_2$), bornite (Cu_5FeS_4), pyrite (FeS_2), galena (PbS), sphalerite (ZnS) and quartz (SiO_2).

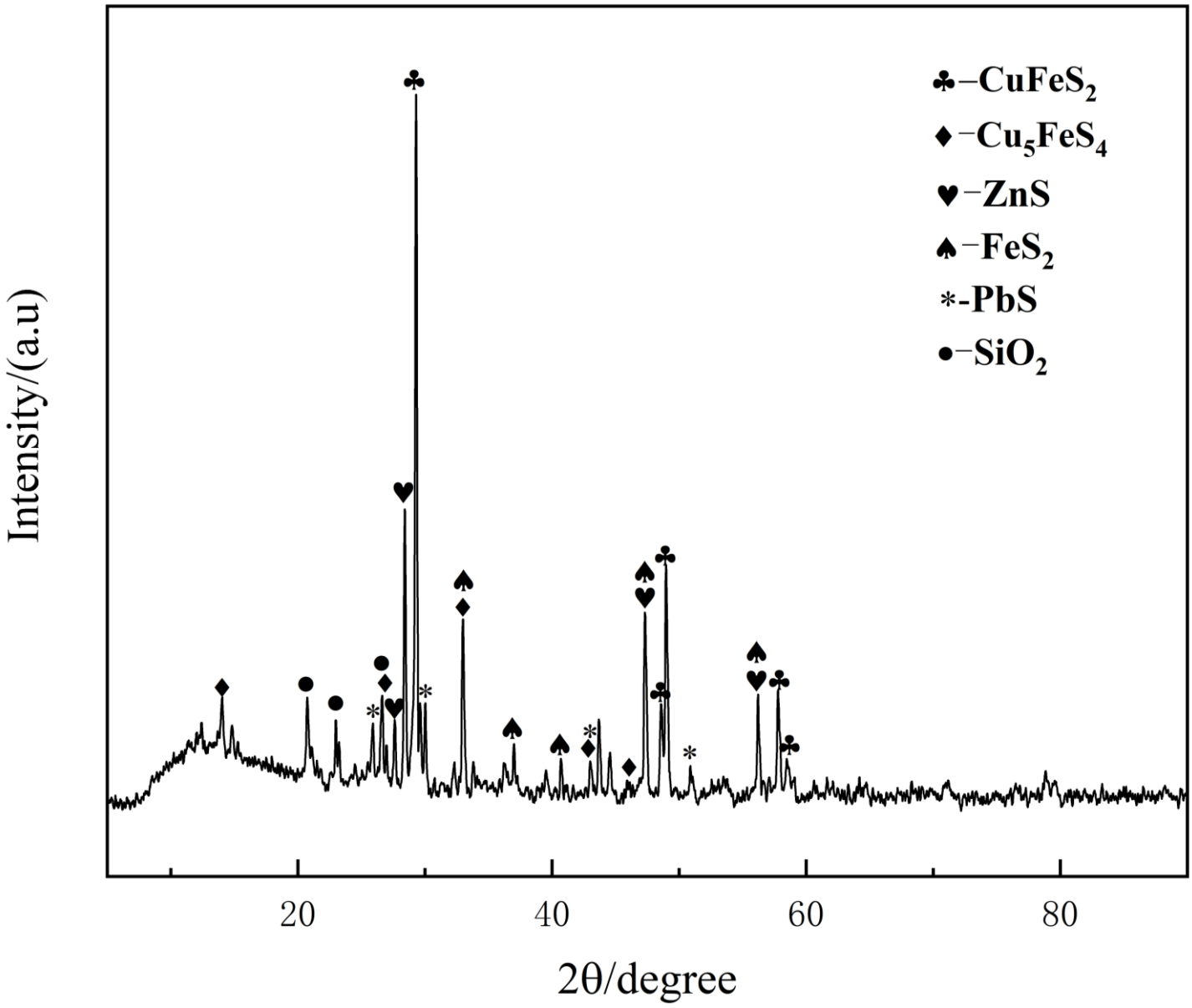

Figure 1 XRD pattern of raw material

2.2.Instruments and experimental method

The effects of reaction temperature, initial acidity, oxygen partial pressure, stirring speed, ultrasonic power and the ratio of liquid to solid on the leaching efficiency of copper and iron and the concentration of sulfuric acid in the reaction system for hydrothermal leaching enhanced by ultrasonic were studied. Firstly, 30 g of the raw material with particle size of -45 μm and the specified volume of water or diluted sulfuric acid according to a specified ratio of liquid to solid were added into the autoclave equipped with ultrasonic irradiation (YZUR-500M, Shanghai Yancheng Instrument Co., LTD.). The mixture was then heated up to the required temperature under

continuous agitation, and oxygen was continuously introduced through a vent value from the oxygen cylinder to maintain a constant pressure and simultaneously ultrasonic with a specified power was induced to react for 4 h. During the leaching process, the concentration of copper, iron and sulfuric acid in the leaching solution was analyzed by sampling at an interval of 15 min for the first two hours and of 30 min for the last two hours. Finally, the autoclave was cooled in the air to the temperature under 50 ℃ and venting out the gas in the autoclave after the experiment was completed, and the obtained pulp was removed and filtered with vacuum filter apparatus to get the leachate and leached residue. The leached residue was dried in oven at 105 ℃ for 2 h prior to further be analyzed. And the obtained leachate was sampled to test the content of copper, zinc, iron and sulfuric acid.

2.3.Analysis and characterization methods

The mineral phase and morphology of the raw material and leached residue obtained were characterized by XRD and scanning electron microscope (SEM, Hitachi Regulus8100). After the raw material and the leached residue were pretreated by dissolving with acid, the chemical composition of the raw material and the leached residue was quantitatively analyzed by inductively coupled plasma emission spectrometry (ICP-AES, Optima-5300DV). The contents of copper, iron and free sulfuric acid in solution were determined by iodimetry, tin (II) reduction-potassium dichromate titration and acid-base neutralization titration, respectively.

The leaching efficiency of copper and iron was calculated according to formula (1).

$$\eta_x = \frac{w_{xi}}{w_{x0}} \times 100\% \quad (1)$$

Where: η_x is the leaching efficiency of copper, zinc and iron; w_{xi} is the mass of copper and iron contained in the leaching solution, and w_{x0} is the mass of copper and iron contained in the raw material.

In addition, during the study of copper leaching kinetics, the leaching efficiency of copper at different times was calculated according to equation (2).

$$X_i = \frac{\left(V_0 - \sum_{i=1}^{i-1} V_i\right) \cdot C_i + \sum_{i=1}^{i-1} V_i \cdot C_i}{W_{xo}} \quad (2)$$

Where: X_i is the copper leaching efficiency at the *i* time of sampling;

V_0 is the total volume of leached liquid before sampling;

V_i is the volume of the *i* sample;

C_i is the concentration of copper in the leaching solution at the *i* time of sampling;

W_{xo} is the mass of copper in the raw material.

3. Results and Discussion

3.1. Leaching mechanism without acid

3.1.1. Thermodynamically feasible and spontaneous of leaching reactions

For indicating thermodynamically feasible and spontaneous of the chemical reaction for realizing leaching valuable metals from CPSSC, it is necessary to calculate the probability of its progress (delta G). In the conditions for leaching valuable metals from CPSSC, the main chemical reactions and their standard Gibbs energy were listed in table 2.

Table 2 The standard Gibbs energy (kJ/mol) of the main chemical reactions in leaching

Chemical reaction	$\Delta_rG^\theta_{298K}$	$\Delta_rG^\theta_{393K}$	$\Delta_rG^\theta_{413K}$	$\Delta_rG^\theta_{433K}$	$\Delta_rG^\theta_{453K}$
$2FeS_2 + 7O_2 + 2H_2O = 2Fe^{2+} + 4H^+ + 4SO_4^{2-}$	-559.887	-513.637	-503.686	-490.798	-477.203
$4FeS_2 + 15O_2 + 2H_2O = 4Fe^{3+} + 4H^+ + 8SO_4^{2-}$	-1162.160	-1052.2	-1029.56	-999.058	-965.251
$FeCuS_2 + 4H^+ + O_2 = Cu^{2+} + Fe^{2+} + 2S^0 + 2H_2O$	-80.899	-63.64	-60.737	-59.304	-56.571
$2ZnS + 4H^+ + O_2 = 2Zn^{2+} + 2S^0 + 2H_2O$	-87.935	-84.557	-82.276	-80.952	-78.443
$2FeS_2 + 4H^+ + O_2 = 2Fe^{2+} + 4S^0 + 2H_2O$	-74.513	-67.331	-64.842	-62.97	-60.989
$2PbS + 4H^+ + 2SO_4^{2-} + O_2 = 2PbSO_4 + 2S^0 + 2H_2O$	-99.773	-103.375	-104.714	-105.528	-106.557
$S^0 + 2H_2O + 3O_2 = 4H^+ + 2SO_4^{2-}$	-288.792	-226.165	-222.128	-216.792	-211.23

From the value of the standard Gibbs energy in table 2, it suggests that chemical reactions of the realized

leaching are thermodynamically feasible and spontaneous as the reason that the standard Gibbs energy ($\Delta_r G_T^\theta$) of these reactions during leaching is minus. Although it is known that chalcopyrite is dissolve in acidic leaching medium, why can water be used as leaching agent in the present work! This because that FeS_2 contained in the CPSSC reacted with water and oxygen to produce sulfuric acid needed to dissolve chalcopyrite, and during the leaching process sulfuric acid could be produced from the oxidation of S^0.

Although sphalerite and galena were contained in CPSSC besides chalcopyrite, it was found in the experimental study under the leaching conditions controlled in this study that galena and sphalerite were easy to react and dissolve. Galena was transformed into lead sulfate or lead alum remained in the leached residue, and zinc contained in the sphalerite was leached in leachate in form of zinc sulfate. Additionally, compared the value of the standard Gibbs energy which ZnS, PbS and $FeCuS_2$ are dissolved in Table 2, it is achieved that $FeCuS_2$ is difficult to be leached than ZnS and PbS. Because the delta G of the leaching reaction of $FeCuS_2$ is the biggest.

3.1.2. Effect of initial concentration of sulfuric acid

Under the conditions of reaction temperature 180 ℃, oxygen partial pressure 0.6 MPa, stirring speed 500 r/min, ultrasonic power 360 W, liquid-solid ratio 10 mL /g, reaction time 4 h and mass ratio of lignosulfonate to raw material 0.2%, the change of copper leaching efficiency with leaching time under different initial sulfuric acid concentrations (without sulfuric acid, acid concentration 5 g/L, 10 g/L, 15 g/L and 20 g/L) were shown in figure 2.

As can be seen from figure 2 that chalcopyrite can be dissolved by maintaining a high sulfuric acid concentration at the initial reaction, and the copper leaching efficiency gradually increases with the increase of initial acidity. When the initial concentration of sulfuric acid was 0 g/L (no sulfuric acid was added, water was used as the lixiviate), the copper leaching efficiency was low in the first 30 min duration, mainly because the leaching reaction of chalcopyrite must involve hydrogen ions, and the increase of acidity was conducive to copper leaching. With the direct oxidation of pyrite (FeS_2) to produce sulfuric acid (see the reaction expressed as equation

(3)), the acidity of the reaction system continues to increase, and the leaching system can provide sufficient acid for the leaching of copper in chalcopyrite.

$$4FeS_2+15O_2+2H_2O=4Fe^{3+}+8SO_4^{2-}+4H^+ \quad (3)$$

It can be demonstrated that the leaching of copper from CPSSC containing pyrite (FeS_2) can be achieved by using water as lixiviate under the conditions of oxygen pressurized atmospheric system.

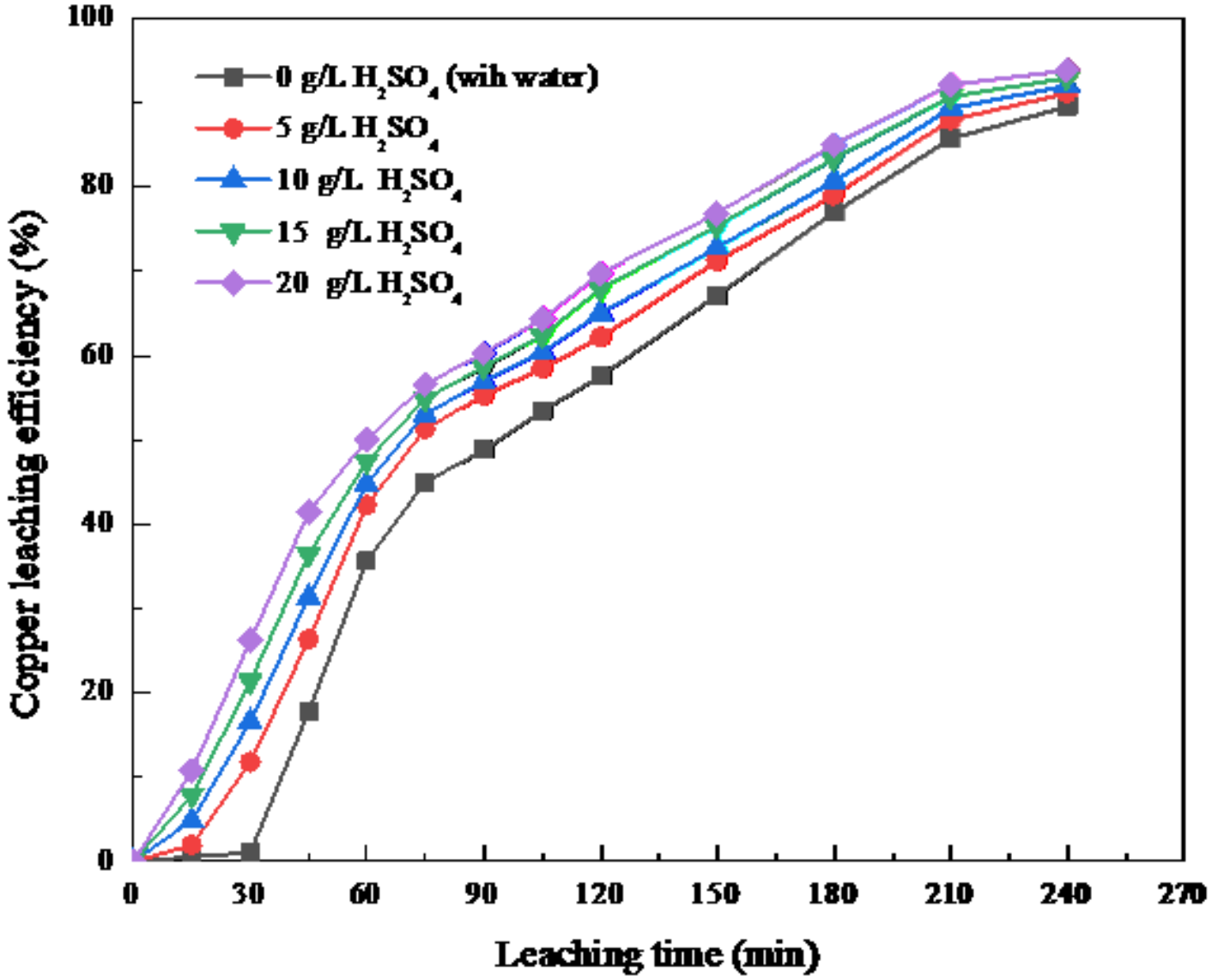

Figure 2 Influence of initial acidity on copper leaching efficiency

3.2. Effects of leaching parameters

3.2.1 Effect of leaching temperature

Under the conditions of water as lixiviate, oxygen partial pressure 0.6 MPa, stirring speed 500 r/min, ultrasonic power 360 W, liquid-solid ratio 10 mL/g, reaction time 4 h, and mass ratio of lignosulfonate to raw material 0.2%, The influence of different leaching temperatures (120 ℃, 140 ℃, 160 ℃, 180 ℃ and 190 ℃) on the leaching efficiency of copper, zinc and iron, as well as the concentration of iron and sulfuric acid in the leaching solution with the leaching time was studied, and the obtained results were shown in figure 3.

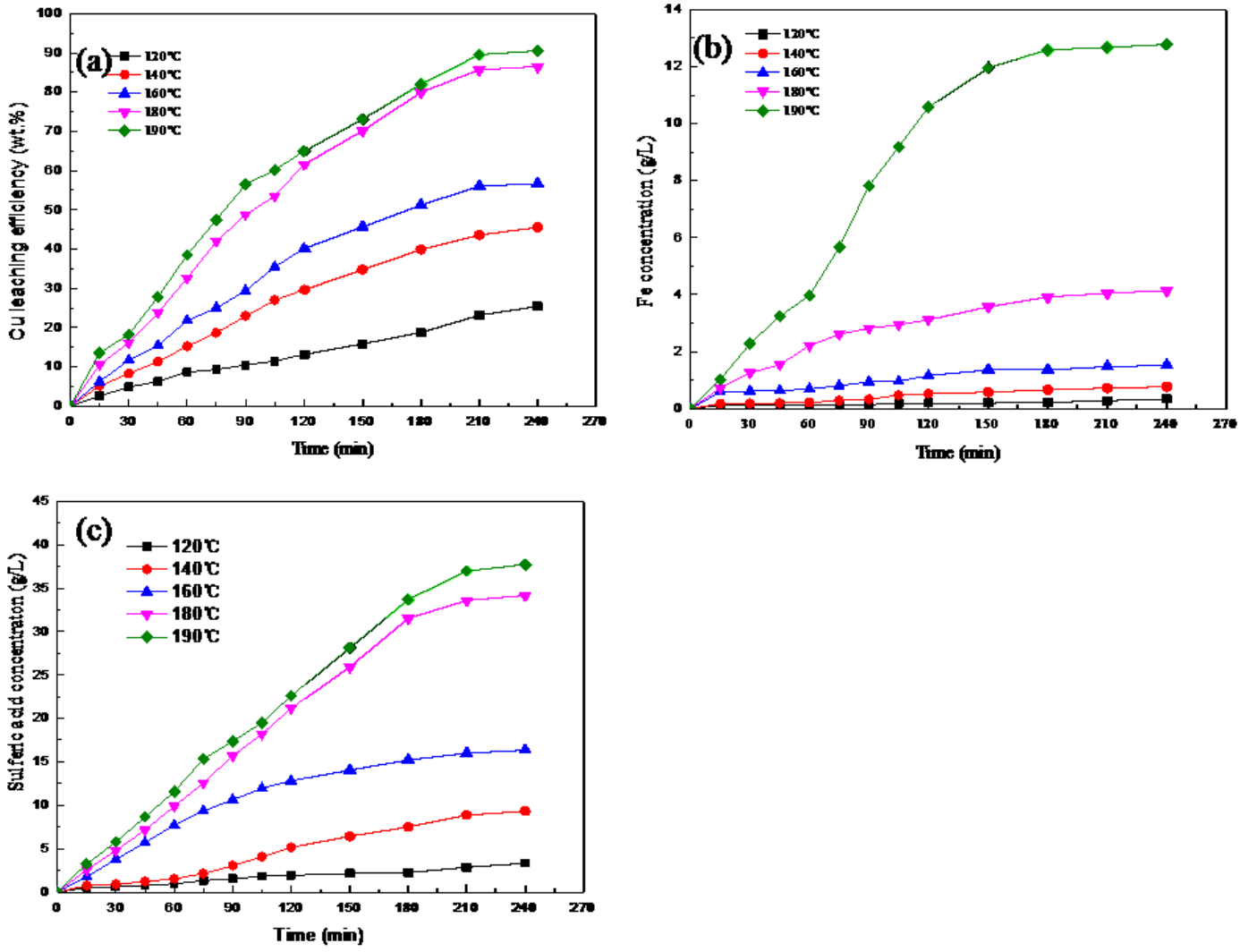

Figure 3 Influence of temperature on leaching process: (a) copper leaching efficiency, (b) iron concentration, and (c) sulfuric acid concentration index leaching for 4 h.

It can be achieved from figure 3 that the leaching efficiency of copper, zinc, and iron, as well as the concentration of iron and sulfuric acid in the leachate increased with the increase of reaction temperature. Under the condition of reaction temperature 120 ℃, pyrite (FeS_2) directly reacts with oxygen and water to produce sulfuric acid at a slow rate, for this reaction is completed insufficient and the residual amount of hydrogen ions generated to react with chalcopyrite, galena, and sphalerite is small, resulting in a low concentration of sulfuric acid in the reaction system and low leaching efficiency of copper and zinc. With the increase of reaction temperature, the oxidation dissolution of pyrite (FeS_2) which can produce sulfuric acid becomes sufficient, the leaching efficiency of copper, zinc and iron increase, resulting from the dissolution of chalcopyrite becoming sufficient, and also the final concentration of sulfuric acid in the leachate increase. Additionally, from figure 2(d) it can be found that the leaching of zinc from CPSSC is easier than that of copper during leaching at the conditions involved in the present work. Only good leaching efficiency of copper can be arrived, the leaching of zinc from CPSSC can be realized. Therefore, the leaching behavior of valuable metals from CPSSC should be focus on the leaching of copper.

XRD analysis of the leached residue (listed in figure 4) shows that there are unreacted chalcopyrite, pyrite and sphalerite in the leached residue obtained at 120 ℃, and the diffraction peaks of the above three substances have become less obvious at 160 ℃, while only plumboferrite, ferric oxide and lead sulfate phases are detected in the leached residue obtained at 180 ℃.

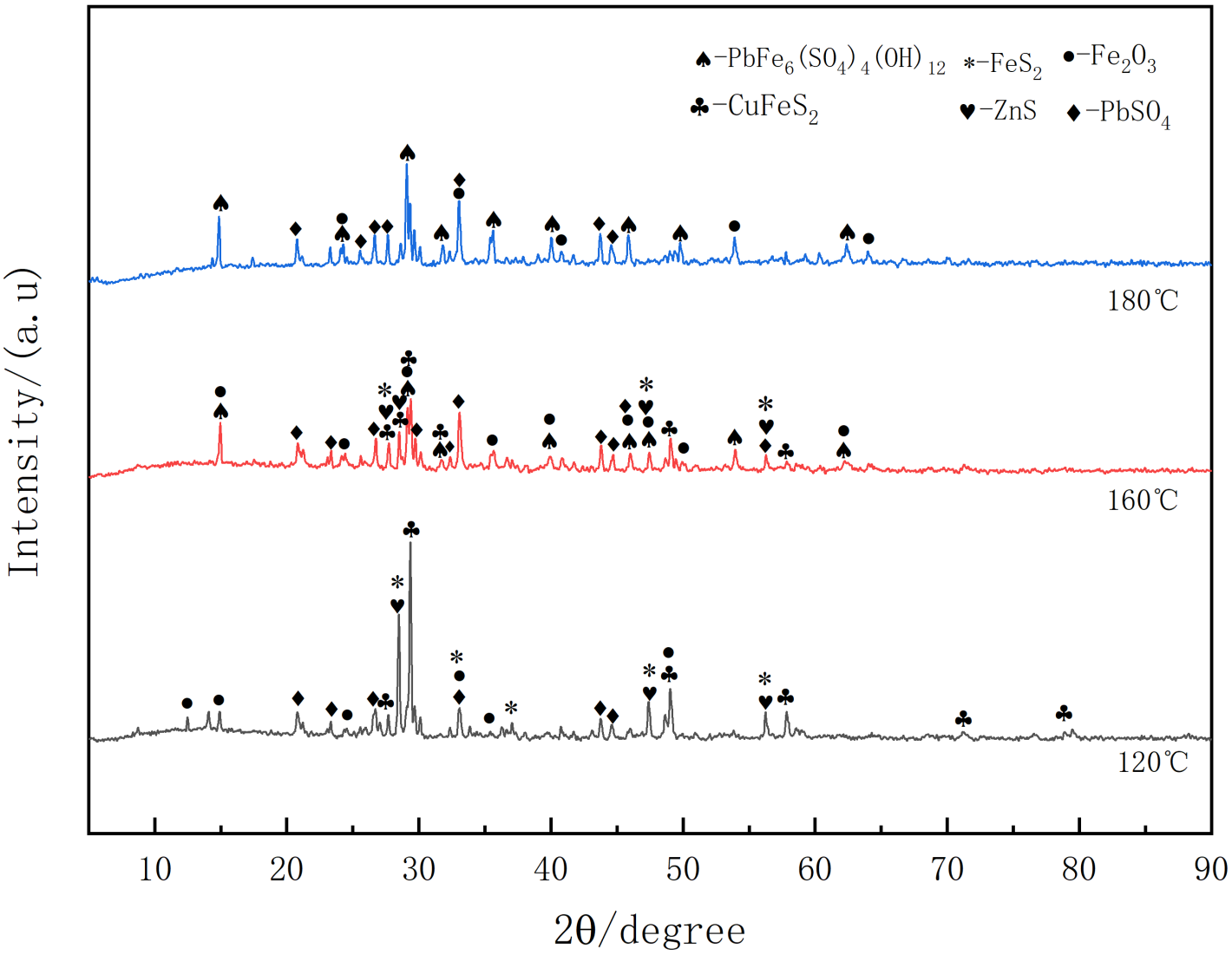

Figure 4 XRD patterns of leached residue at different temperatures

The leached residues at different reaction temperatures were analyzed by SEM/EDS, and the obtained results were shown in figure 5 and figure 6. It can be seen in figure 5 that Cu exists in the leached residue while leaching at 160 ℃, and combined with XRD data (figure 4), it can be demonstrated that the leaching reaction is incomplete, and the surface of the leached residue obtained is coated with the reaction products plumboferrite and hematite. As shown in figure 6, the leaching reaction was completed at 180 ℃, and the main components of the leached residue obtained were hematite, lead sulfate and a small amount of plumboferrite. These experimental results showed that increasing the reaction temperature was beneficial to the leaching reaction, leading to the mineral phases in the leached residue obtained mainly existed into hematite and lead sulfate.

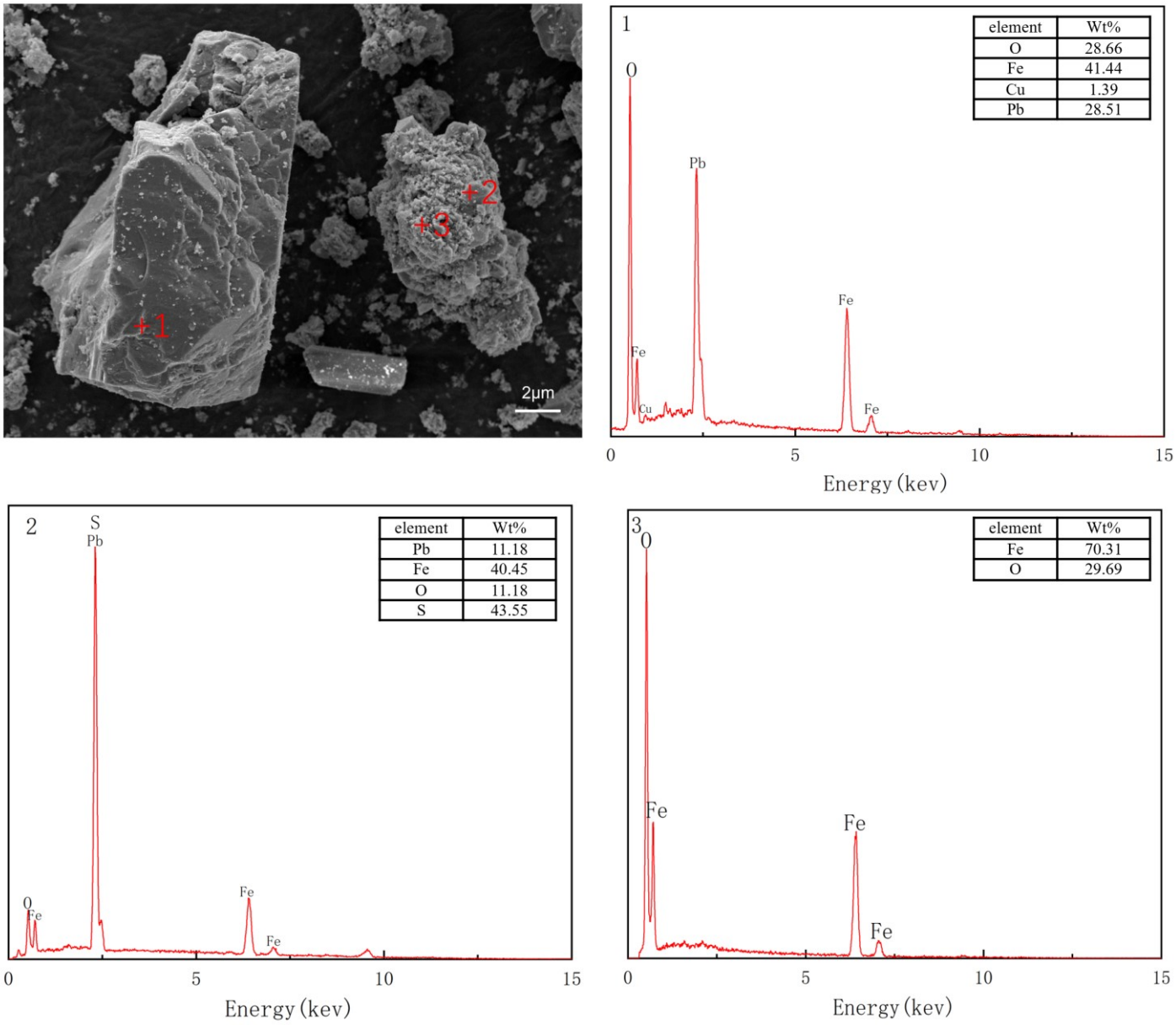

Figure 5 SEM-EDS spectra of leached residue at 160 ℃

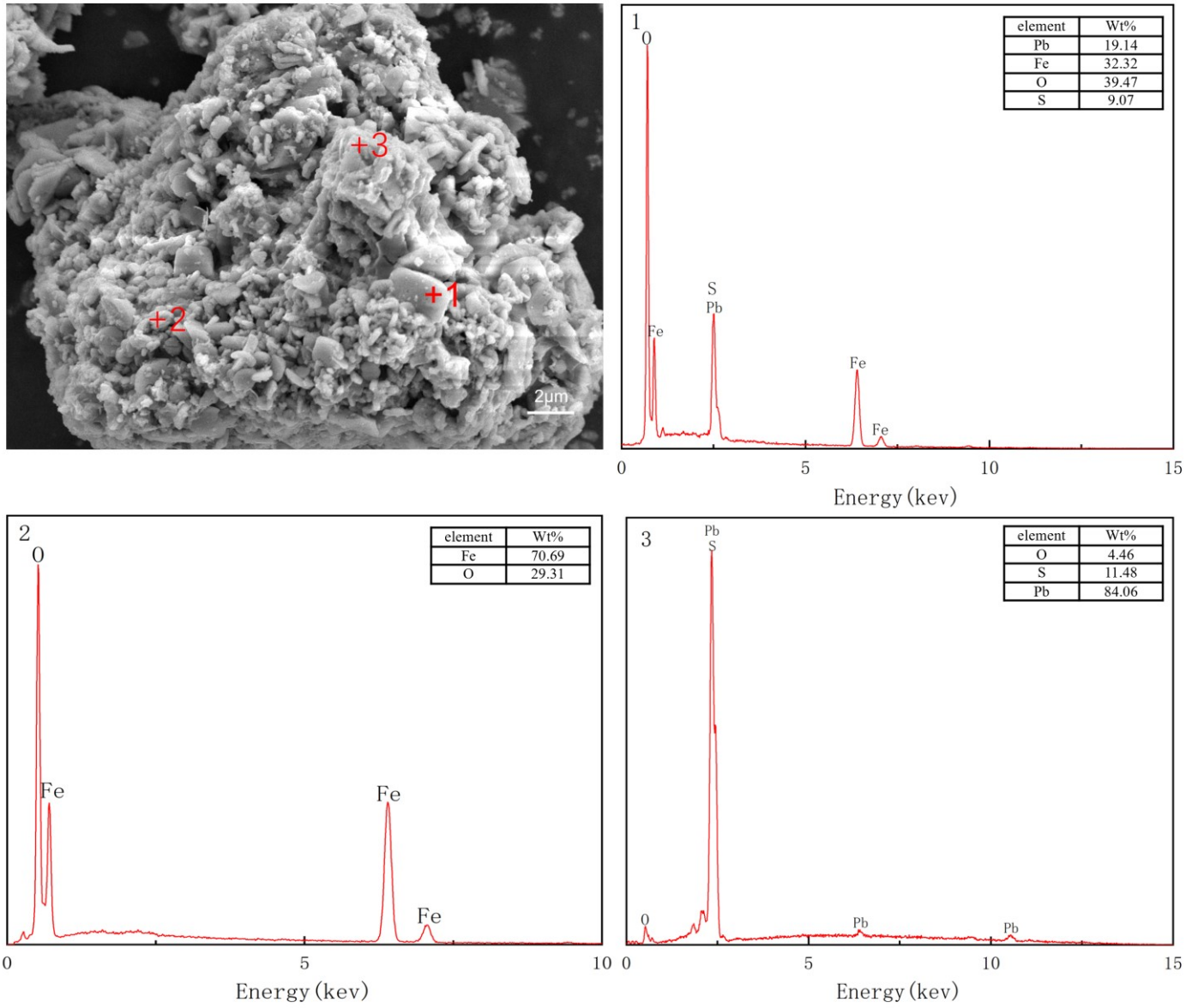

Figure 6 SEM-EDS spectra of leached residue at 180 ℃

3.2.2. Effect of oxygen partial pressure

Under the conditions of reaction temperature 180 ℃, water as lixiviate, stirring speed 500 r/min, ultrasonic power 360 W, liquid-solid ratio 10 mL/g, reaction time 4 h and mass ratio of sodium lignosulfonate to raw material as 0.2%, the effects of different oxygen partial pressures (0.4, 0.6, 0.8, 1.0 and 1.2 MPa) on the copper leaching efficiency were shown in figure 7.

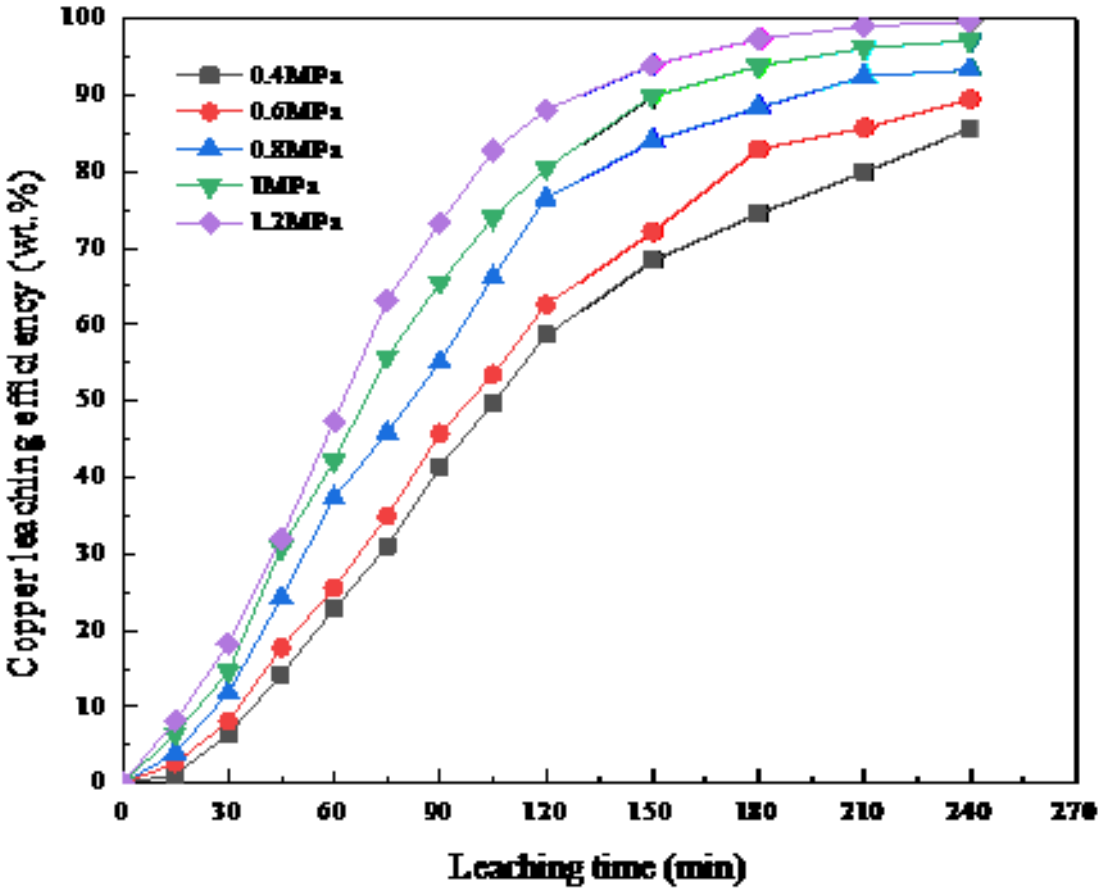

Figure 7 Influence of oxygen partial pressure on copper leaching efficiency

Figure 7 shows that the leaching efficiency of copper increases with the increasing oxygen partial pressure in the range of 0.4-1.2 MPa. But the growth rate of copper leaching efficiency in the range of 0.4-1.0 MPa is bigger than that of during the rage between 1.0-1.2 MPa. This is mainly because increasing the partial pressure of oxygen is conducive to increasing the dissolved oxygen in the leaching solution, thus accelerating the oxidation and dissolution of minerals such as pyrite (FeS_2) and chalcopyrite in the raw materials. However, when the oxygen partial pressure increases to a certain extent, the concentration of dissolved oxygen in the leaching solution gradually reaches saturation, so the influence of copper leaching efficiency on the increase of oxygen partial pressure is not significant. The high oxygen partial pressure leads to the conversion of sulfur in the sulfide into sulfuric acid, and the acidity in the solution increases, limiting the hydrolysis of iron ions and increasing the leaching efficiency of iron in the solution. It is also found that the iron content in the leaching solution increased with the increase of the iron leaching efficiency in the range of 1.0-1.2 MPa oxygen partial pressure. However,

the high partial pressure of oxygen will raise higher requirements for the manufacturing of equipment used for leaching, increasing the investment while this process further applied in future. The optimal partial pressure of oxygen is determined as 1.0 MPa.

3.2.3. Effect of stirring speed

Under the conditions of reaction temperature 180 ℃, water as lixiviate, oxygen partial pressure 1.0 MPa, ultrasonic power 360 W, liquid-solid ratio 10 mL/g, reaction time 4 h and mass ratio of sodium lignosulfonate to raw material 0.2%, the effects of different stirring speed (300, 400, 500, 600 and 700 r/min) on the copper leaching efficiency were shown in figure 8.

As shown in figure 8, in the stirring speed range of 300 r/min to 600 r/min, the copper leaching efficiency increases with the stirring speed. There are two reasons accounting for this phenomenon. One is that enhancing agitation can make the distribution of minerals in the leaching solution more uniform and the contact between reactants more adequate. The other one is that the high stirring speed can help to improve the diffusion of oxygen and hydrogen ions. In addition, after the stirring speed exceeds 600 r/min, the concentration of hydrogen ions and oxygen concentrations on the surface of chalcopyrite has gradually reached saturation, so strengthening the diffusion of oxygen and hydrogen ions can no longer improve the oxidation reaction of chalcopyrite. Moreover, the leaching efficiency of copper does not increase significantly in the stirring speed range of 600 r/min to 700 r/min. It can be arrived that strengthening agitation can not only promote the oxidation reaction of chalcopyrite, but also promote the dissociation of pyrite and the oxidation reaction of sulfur during the leaching process, resulting in a continuous increase in the acidity of the leaching solution, a decrease in the hydrolysis rate of iron ions, and finally a continuous increase in the leaching rate of iron ions, the optimal stirring speed is chosen as 600 r/min.

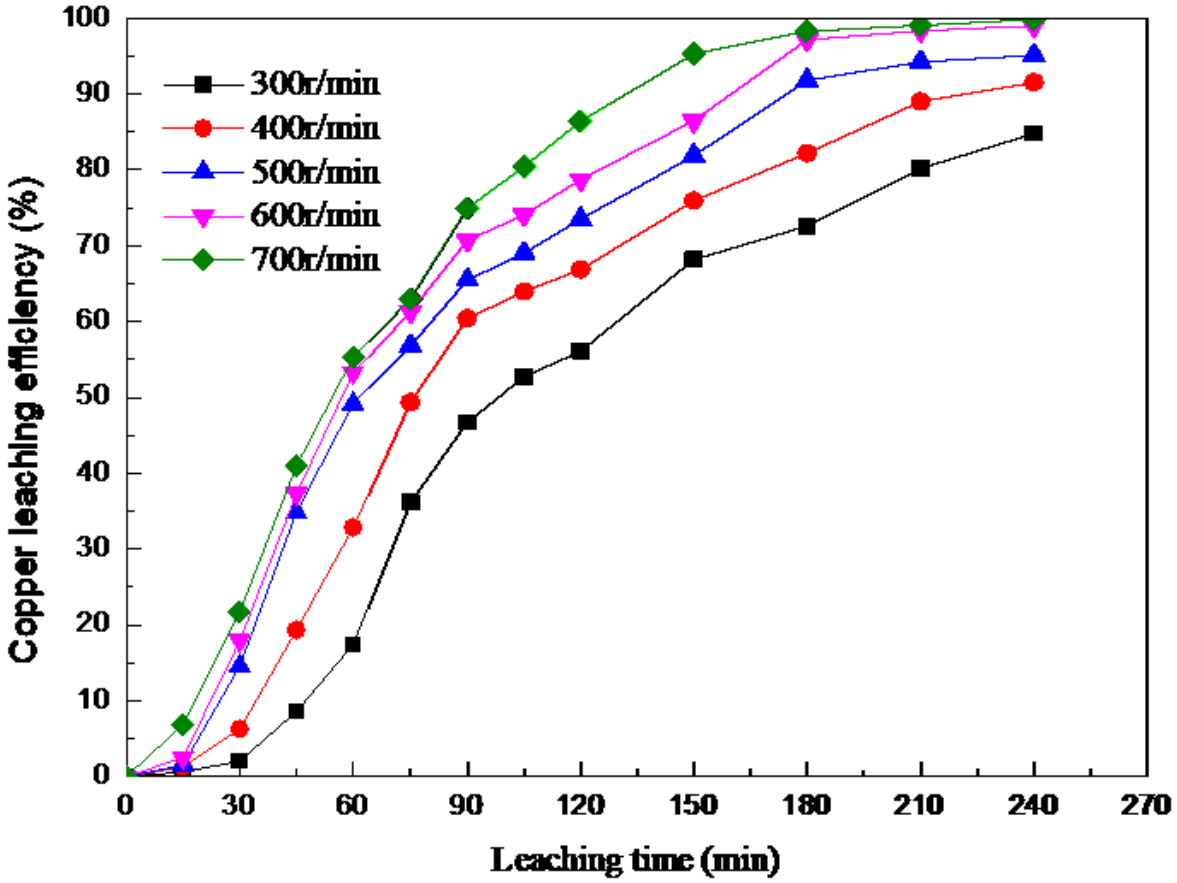

Figure 8 Influence of stirring speed on copper leaching efficiency

3.2.4. Effect of ultrasonic power

Under the conditions of reaction temperature 180 ℃, water as lixiviate, oxygen partial pressure 1.0 MPa, stirring speed 600 r/min, liquid-solid ratio 10 mL/g, reaction time 4 h and mass ratio of sodium lignosulfonate to raw material 0.2%, the effects of without ultrasound and with different ultrasonic power (90, 180, 270, 360 and 450 W) on the copper leaching efficiency and the morphology of leached residue were shown in figure 9 and figure 10 respectively.

Figure 9 shows that the copper leaching efficiency increases with the increase of the ultrasonic power when the ultrasonic power is below 360 W. And figure 10 shows that the particle of the obtained leached residue is small and porosity and it is covered with reaction products on its surface with the increase of ultrasonic power demonstrating the leaching reaction is more adequate. In addition, the particle distribution analysis of leached residues enhanced by ultrasonic with power at 0 W, 180 W and 360 W was performed on laser particle size

analyzer (Malvern Mastersizer 3000, Great Britain), with the obtained data of Dv (90) was 16.636, 12.902 and 11.136 μm respectively. The reason for the above phenomenon is that the cavitation effect of ultrasonic wave and the extreme environment of high temperature and high pressure in micro-area are generated, which catalyzes the strengthening of chemical reaction and improves the leaching efficiency of copper [29,30]. In addition, it can be seen from the experimental results in figure 8 that the copper leaching efficiency no longer increases significantly with the increase of ultrasonic power while the ultrasonic power exceeds 360 W. This phenomenon is due to the fact that with the further increase of ultrasonic power, too concentrated holes will be formed near the ultrasonic generation probe, which will affect the conduction of sonic waves, weaken the strengthening effect, and ultimately lead to the reduction of reaction efficiency [31,32]. The optimal ultrasonic power is determined as 360 W.

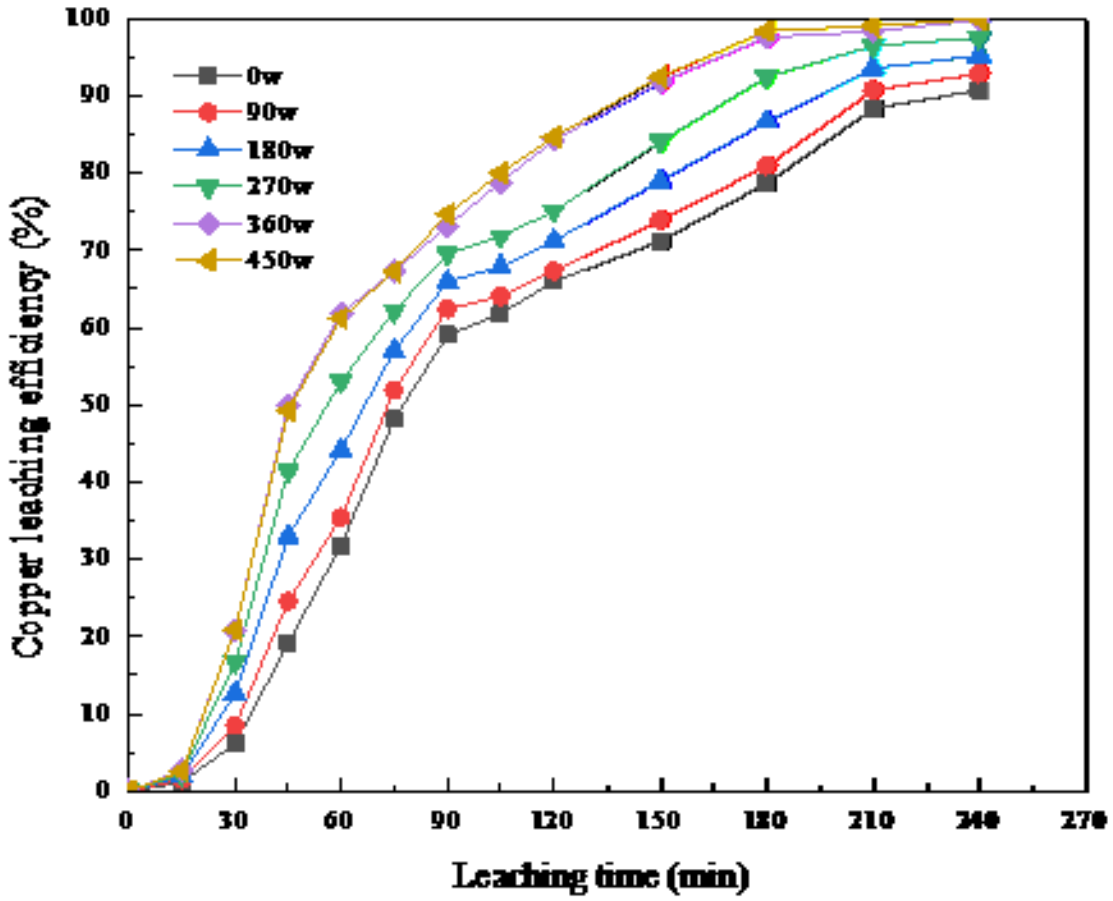

Figure 9 Influence of ultrasonic power on copper leaching efficiency

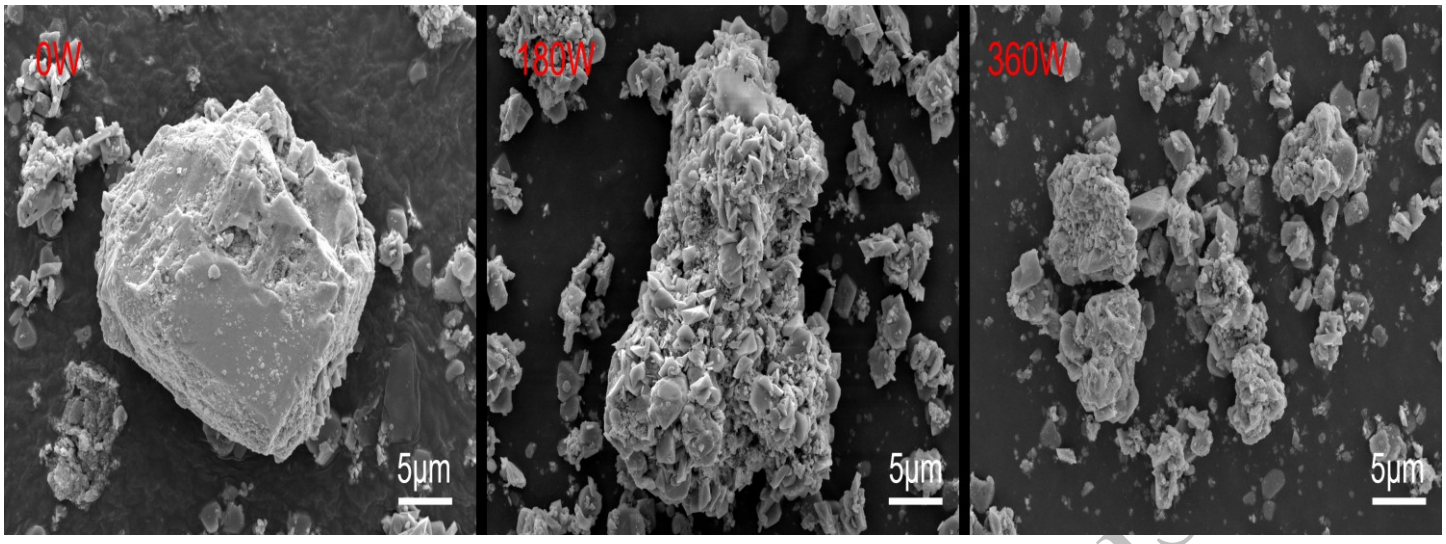

Figure 10 SEM images of leached residue under different ultrasonic power

3.23. **Leaching behavior under optimal conditions**

The raw material was added into the autoclave equipped with ultrasonic irradiation for hydrothermal leaching enhanced by ultrasonic under the optimal conditions determined as above. Which reaction temperature was 180 ℃, water as lixiviate, oxygen partial pressure was 1.0 MPa, stirring speed was 600 r/min, liquid-solid ratio was 10 mL/g, and mass ratio of sodium lignosulfonate to raw material was 0.2%, for reacting 4 h by irradiated with ultrasonic power of 360 W, the average results of three parallel experiments was that the leaching efficiency of copper and iron are 99.12% and 19.64%, respectively. Moreover, the leaching efficiency of copper with ultrasonic irradiation was increased by 10.02% from that of without ultrasonic irradiation, and the leaching efficiency of iron with ultrasonic irradiation was decreased by 5.20% from that of without ultrasonic irradiation.

3.3 Copper leaching kinetic analysis

3.3.1 Choice and determination of kinetics model

It is necessary for kinetic analysis of leaching process to select the kinetic model. According to the preliminary analysis, the leaching process of the CPSSC belongs to the gas-liquid-solid multiphase reaction. Through the analysis of the chemical reaction occurring in the leaching process, it can be seen that solid phase products such as hematite, sulfur elemental and plumboferrite will be generated during the reaction process,

which are easily coated on the surface of unreacted chalcopyrite. Therefore, the kinetic analysis of the hydrothermal leaching process under oxygen pressure enhanced with ultrasonic field was carried out using the unreacted core shrinkage model [33-34]. According to the theory of the model, there are three kinds of chemical reaction speed control steps, which are chemical reaction control, internal diffusion control and mixed control which are jointly determined by two factors. The specific rate equations were listed as equation (4), (5) and (6).

$$1 - (1-X)^{1/3} = K_r t \quad (4)$$

$$1- 2/3X- (1-X)^{2/3} = K_d t \quad (5)$$

$$1-(1-X)^{1/3}-1/3\ln(1-X) = K_m t \quad (6)$$

Where X is the copper leaching efficiency, t is the reaction time, K_r, K_d and K_m are the apparent rate constants of chemical reaction control, internal diffusion control and mixing control, respectively.

The data in figure 3(a) were substituted into equations (4), (5) and (6) respectively for linear fitting, and the obtained results were shown in figure 11. And figure 11 shows that the correlation coefficients of chemical reaction control and mixing control fitting are close to 1, indicating that the hydrothermal leaching process under oxygen pressure of CPSSC enhanced in the ultrasonic field conforms to both chemical reaction control and mixing control models.

The reaction rate constants of chemical reaction control and mixing control fitted at different temperatures were substituted into the Arrhenius equation to obtain the apparent activation energy. The Arrhenius equation was listed inequation (7).

$$K = Ae^{(-E/RT)} \quad (7)$$

Where A is the frequency factor, E is the apparent activation energy (kJ/mol), R is the gas equilibrium constant (8.314 J/mol), and T is the thermodynamic temperature (K).

Equation (8) could be obtained by taking logarithm of both sides of equation (7):

$$\ln K = -E/RT + \ln A \quad (8)$$

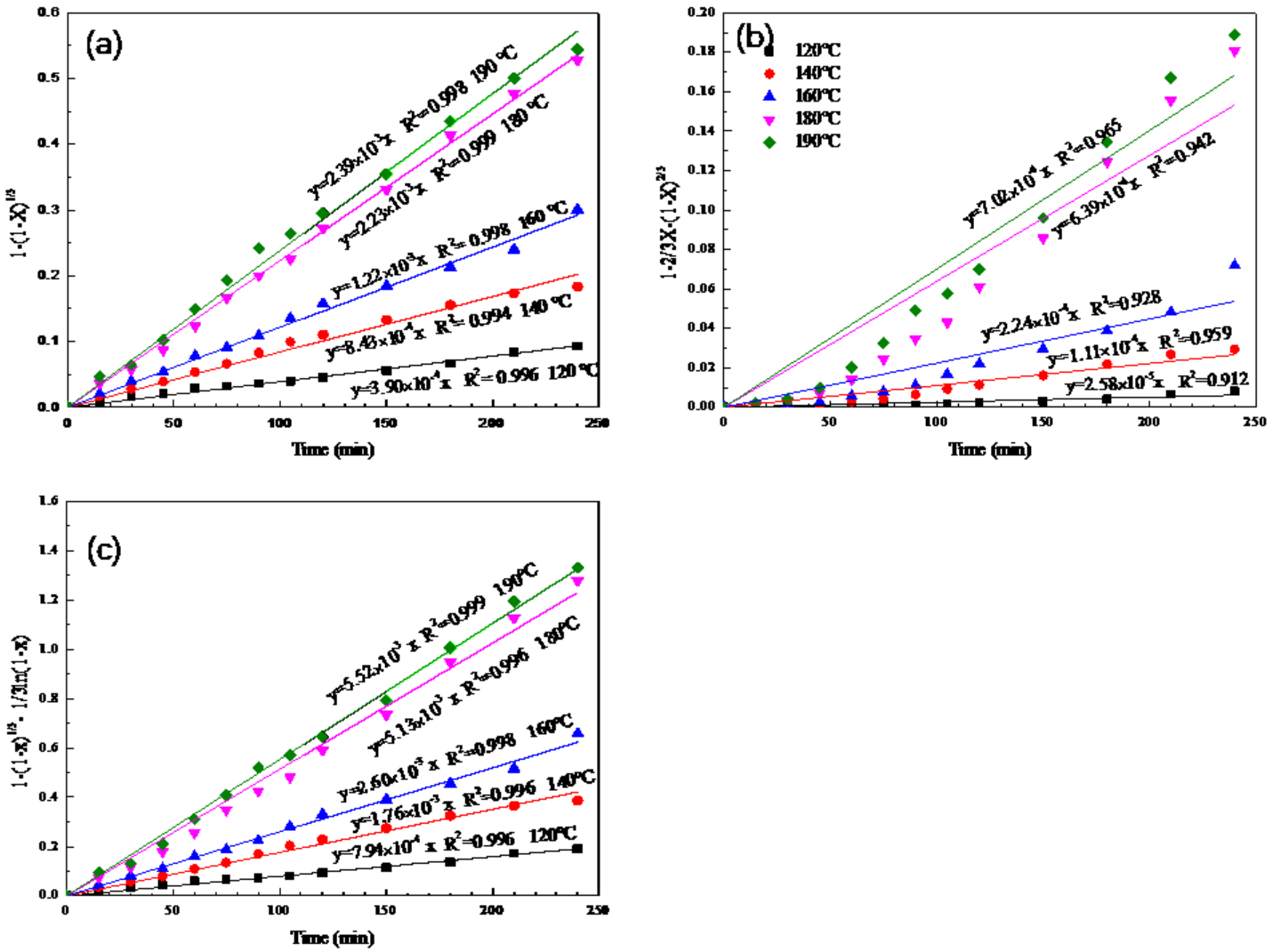

Figure 11 Fitting results of control model: (a) chemical reaction control, (b) internal diffusion control and (c) mixing control

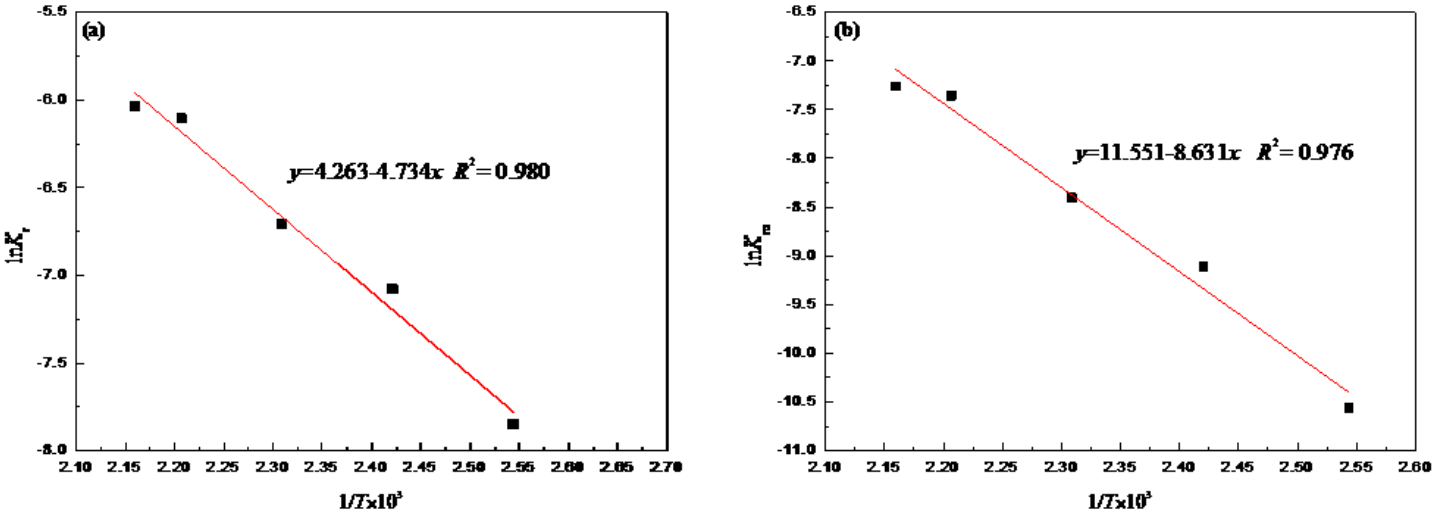

Figure 12 Relationship between *lnK* and 1/*T* at different control model: (a) chemical reaction control, (b)

mixing control

ln$K$ was used to plot versus 1/T (figure 12) and linear fitting was performed. The apparent activation energy (E) of the chemical reaction control and mixing control was 39.36 kJ/mol and 71.76 kJ/mol, respectively, and the frequency factor A was 71.02 and 1.039×10^5, respectively. Since the activation energy controlled by the chemical reaction was greater than 41.8 kJ/mol [35-38], it was further indicated that hydrothermal leaching of CPSSC enhanced by ultrasonic under oxygen pressure belongs to mixing control model, and its kinetic equation could be expressed as equation (9).

$$1-(1-X)^{1/3}-1/3\ln(1-X) = 1.039\times10^5 e^{[-71760/(RT)]}t \quad (9)$$

3.3.2 Kinetics equation deduction

On the basis of determining the kinetic equation of the leaching reaction, the effects of ultrasonic power, oxygen partial pressure and stirring speed on the leaching process were quantitatively analyzed. The relationship between copper leaching efficiency and time in the mixed control process could be expressed by the macroscopic dynamic equation of equation (10) [39].

$$1-(1-X)^{1/3}-1/3\ln(1-X) = k' P_{O_2}^{n_1} r^{n_2} P^{n_3} e^{[-E/(RT)]}t \quad (10)$$

where P is ultrasonic power (W), P_{O_2} is the partial pressure of oxygen (MPa), r is stirring speed (r/min), k' is the temperature dependent constant, and n_1, n_2, n_3 are the reaction order of ultrasonic power, oxygen partial pressure and stirring speed, respectively

3.3.2.1 Reaction order of oxygen partial pressure

Leaching data related to oxygen partial pressure (figure 7) were brought into the dynamic equation of hybrid control for linear fitting, and the fitting results were shown in figure 13(a). The natural logarithm (lnK_m) of constant velocity K_m obtained in the range of 0.4-1.2 MPa was plotted against the natural logarithm (lnP_{O2}) of oxygen partial pressure (figure13(b)), and linear fitting was carried out, resulting in the reaction order (n_1) of oxygen partial pressure was obtained as 0.771.

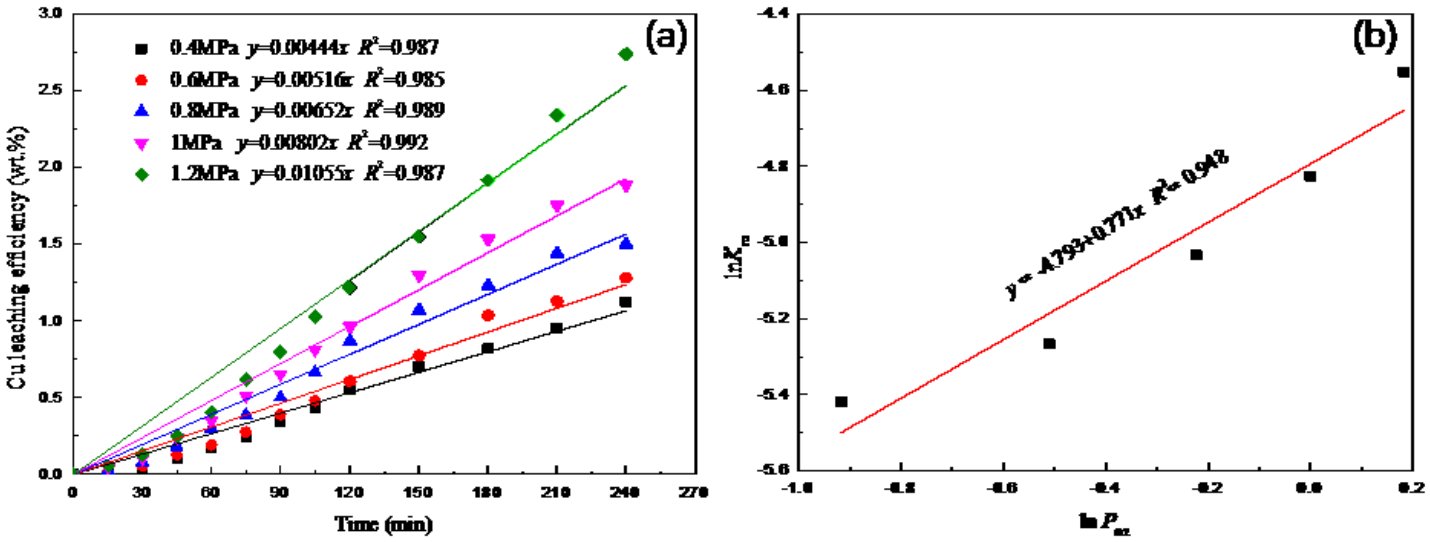

Figure 13 (a) Fitting results of mixing control models under different oxygen partial pressures and (b) fitting results of ln$K$ and lnP_{O_2} at different oxygen partial pressures during leaching

3.3.2.2 Reaction order of stirring speed

Leaching data related to stirring speed (figure 8) were brought into the dynamic equation of mixing control for linear fitting, and the fitting results were shown in figure 14(a). The natural logarithm (lnK_m) of constant speed K_m obtained within the range of 300 to 600 r/min was plotted against the natural logarithm (ln$r$) of stirring speed (see figure 14(b)), and linear fitting was carried out, resulting in the reaction order (n_2) of stirring speed was obtained as 0.903.

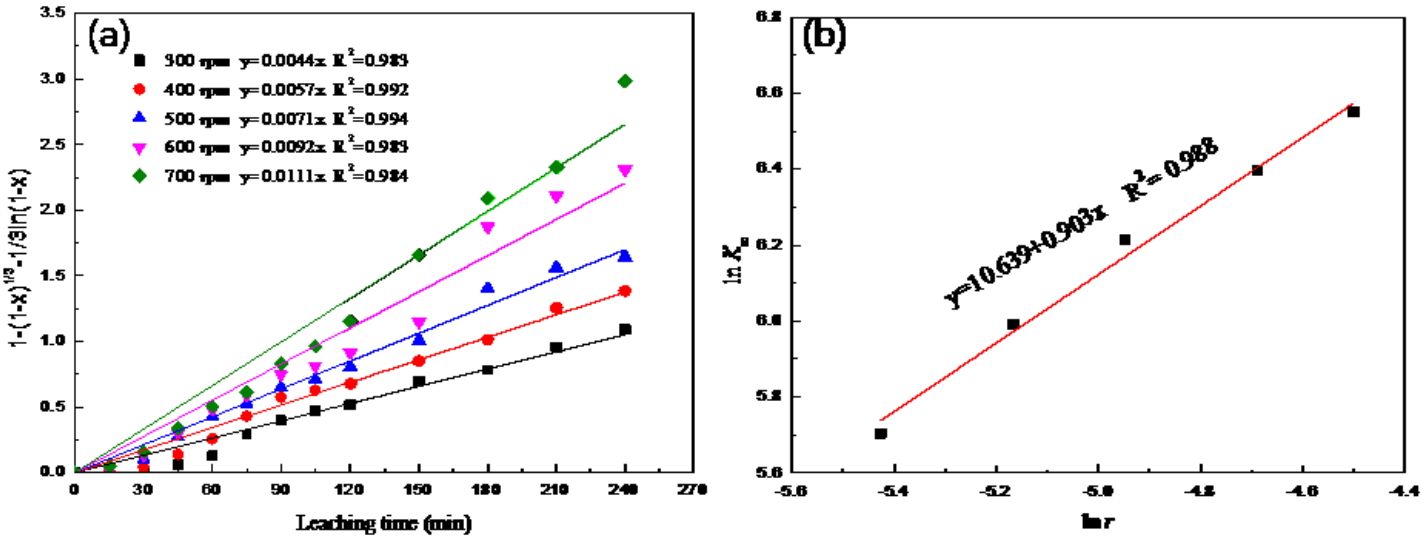

Figure 14 Fitting results of mixing control model at different stirring speeds (a) and results of ln *k* and ln *r* at different stirring speeds during leaching (b).

3.3.2.3 Reaction order of ultrasonic power

Leaching data related to ultrasonic power (figure 9) were brought into the dynamic equation of hybrid control for linear fitting, and the fitting results were shown in fiugre 15(a). The natural logarithm (lnK_m) of constant speed K_m obtained from 90 W to 450 W was plotted against the natural logarithm (ln$P$) of ultrasonic power P, and the linear fitting was carried out. The results were shown in figure 15(b), and the reaction order (n_3) of ultrasonic power was calculated to be 0.431.

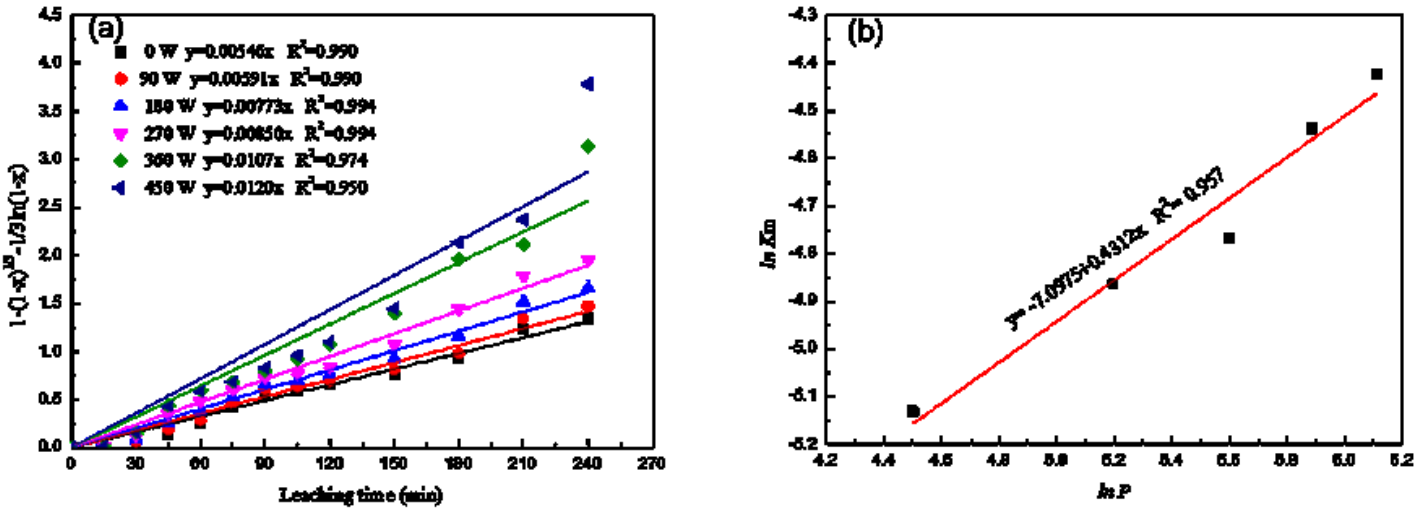

Figure 15 (a) Fitting results of mixing control under different ultrasonic powers and (b) relationship

between lnK_m and ln$P$ in leaching process

By bringing the corresponding reaction order obtained into the kinetic equation, the macroscopic kinetic equation was expressed as follows: $1-(1-X)^{1/3}-1/3\ln(1-X) = 40.457P_{O_2}^{0.771}r^{0.903}P^{0.431}e^{(-8630.19/T)}t$。

4. Conclusion

1) With water as lixiviate (none acid was added during the leaching process), the hydrothermal leaching enhanced with ultrasonic can eco-friendly utilize CPSSC for selective extraction copper, and under the conditions of reaction temperature 180 ℃, oxygen partial pressure 1.0 MPa, stirring rate 600 r/min, ultrasonic power 360 W, liquid solid ratio 10:1 and mass ratio of sodium lignosulfonate to raw material 0.2%, the leaching efficiency of copper from CPSSC reached 99.12%, simultaneously the leaching efficiency of iron was only 19.64%.

2) The enhancing by ultrasonic resulted in the extraction efficiency of copper increased by 10.02% and the leaching efficiency of iron decreased by 5.20%, demonstrating a selective extraction of copper.

3) Kinetics study of the leaching process showed that the leaching process of copper from CPSSC was in line with the unreacted shrinkage core model and belonged to mixing control. The apparent activation energy of the leaching reaction was 71.76 kJ/mol, and the macroscopic kinetic equation of the leaching reaction could be expressed as $1-(1-X)^{1/3}-1/3\ln(1-X) = 40.457P_{O_2}^{0.771}r^{0.903}P^{0.431}e^{(-8630.19/T)}t$.

Acknowledgments

The authors express the sincere appreciation to the National Natural Science Foundation of China for the financial support (Project No. 21978122).

Declaration of interest statement

This article has not been published elsewhere in whole or in part. All authors have read and approved the content, and agree to submit for consideration for publication in the journal. There are no any ethical/legal

conflicts involved in the article.

References

[1] J. X. Hu, G. C. Tian, F. T. Zi, X. Z. Hu, Leaching of chalcopyrite with hydrogen peroxide in 1-hexyl-3-methyl-imidazolium hydrogen sulfate ionic liquid aqueous solution, Hydrometallurgy. 169 (2017) 1-8. https://doi.org/10.1016/j.hydromet.2016.12.001

[2] R. T. Jones, Electronic structures of the sulfide minerals sphalerite, wurtzite, pyrite, marcasite, and chalcopyrite. (eds) Adelaide: University of South Australia, (2006) 5-80.

[3] H. Nourmohamadi, M. D. Esrafili, V. Aghazadeh, DFT study of ferric ion interaction with passive layer on chalcopyrite surface: Elemental sulfur, defective sulfur and replacement of M^{2+} (M=Cu and Fe) ions, Computational Condensed Matter, 26 (2021) e00536. https://doi.org/ 10.1016/j.cocom.2021.e00536

[4] S. F. Wu, C. R. Yang, W. Q. Qin, F. Jiao, J. Wang, Y. S. Zhang, Sulfur composition on surface of chalcopyrite during its bioleaching at 50 °C, Transactions of Nonferrous Metals Society of China, 25(12) (2015) 4110-4118. https://doi.org/10.1016/S1003-6326(15)64062-6

[5] G. Mucsi, A review on mechanical activation and mechanical alloying in stirred media mill, Chemical Engineering Research and Design, 148 (2019) 460-474. https://doi.org/10.1016/j.cherd.2019.06.029

[6] S. X. Zhao, G. R. Wang, H. Y. Yang, G. B. Chen, X. M. Qiu. Agglomeration-aggregation and leaching properties of mechanically activated chalcopyrite, Transactions of Nonferrous Metals Society of China, 31(5) (2021) 1465-1474. https://doi.org/10.1016/S1003-6326(21)65590-5

[7] K. Maryam, B. Rezai, A. A. Abdollahzadeh, B. P. Wilson, M. Molaeinasab, M. Lundström, Investigation into the effect of mechanical activation on the leaching of chalcopyrite in a glycine medium, Hydrometallurgy, 203 (2021) 105492. https://doi.org/10.1016/j.hydromet.2020.105492

[8] X. B. Wan, J. J. Shi, T. Pekka, A. Jokilaakso, Extraction of copper from copper-bearing materials by sulfation roasting with SO_2-O_2 Gas, JOM, 72(10) (2020) 3436-3446. https://doi.org/10.1007/s11837-020-

04300-7

[9] S. D. Lin, L. Gao, Y. Yang, J. Chen, S. H. Guo, M. Omran, G. Chen, Dielectric properties and high temperature thermochemical properties of the pyrolusite-pyrite mixture during reduction roasting, Journal of Materials Research and Technology, 9(6) (2020) 13128-13136. https://doi.org/10.1016/j.jmrt.2020.09.056

[10] Y. L. Bai, W. Wang, K. W. Dong, F. Xie, D. K. Lu, Y. F. Chang, K. X. Jiang, Effect of microwave pretreatment on chalcopyrite dissolution in acid solution, Journal of Materials Research and Technology, 16 (2022) 471-481. https://doi.org/10.1016/j.jmrt.2021.12.014

[11] M. X. Hong, X. T. Huang, X. W. Gan, G. Z. Qiu, J. Wang, The use of pyrite to control redox potential to enhance chalcopyrite bioleaching in the presence of leptospirillum ferriphilum, Minerals Engineering, 172 (2021) 107145. https://doi.org/10.1016/j.mineng.2021.107145

[12] Z. Y. Tian, H. D. Li, Q. Wei, W. Q. Qin, C. R. Yang, Effects of redox potential on chalcopyrite leaching: An overview, Minerals Engineering, 172 (2021) 107135. https://doi.org/10.1016/j.mineng.2021.107135

[13] L. Li, M. Soleymani, A. Ghahreman, New insights on the role of lattice-substituted silver in catalytic oxidation of chalcopyrite, Electrochimica Acta, 369 (2020) 137652. https://doi.org/10.1016/j.electacta.2020.137652

[14] R. Liao, X. X. Wang, B. J. Yang, M. X. Hong, H. B. Zhao, J. Wang, G. Z. Qiu, Catalytic effect of silver-bearing solid waste on chalcopyrite bioleaching: A kinetic study, Journal of Central South University, 27(5) (2020) 1395-1403. https://doi.org/10.1007/s11771-020-4375-1

[15] K. T. Konadu, R. Sakai, D. M. Mendoza, C. Chuaicham, H. Miki, K. Sasaki, Effect of carbonaceous matter on bioleaching of Cu from chalcopyrite ore, Hydrometallurgy, 195 (2020) 105363. https://doi.org/10.1016/j.hydromet.2020.105363

[16] M. Kartal, F. Xia, D. Ralph, W. D. A. Rickard, F. Renard, W. Li, Enhancing chalcopyrite leaching by tetrachloroethylene-assisted removal of sulphur passivation and the mechanism of jarosite formation,

Hydrometallurgy, 191 (2020) 105192. https://doi.org/10.1016/j.hydromet.2019.105192

[17] T. Wen, Y. L. Zhao, Q. H. Xiao, Q. L. Ma, S. C. Kang, H. Q. Li, S. X. Song, Effect of microwave-assisted heating on chalcopyrite leaching of kinetics, interface temperature and surface energy, Results in Physics, 7 (2017) 2594-2600. https://doi.org/10.1016/j.rinp.2017.07.035

[18] T. Wen, Y. L. Zhao, Q. L. Ma, Q. H. Xiao, T. T. Zhang, J. X. Chen, S. X. Song, Microwave improving copper extraction from chalcopyrite through modifying the surface structure, Journal of Materials Research and Technology, ,9(1) (2020) 263-270. https://doi.org/10.1016/j.jmrt.2019.10.054

[19] J. Cháidez, J. Parga, J. Valenzuela, R. Carrillo, I. Almaguer, Leaching chalcopyrite concentrate with oxygen and sulfuric acid using a low-pressure reactor, Metals, 9(2) (2019) 189. https://doi.org/10.3390/met9020189

[20] J. J. Xi, Y. L. Liao, G. X. Ji, Q. F. Liu, Y. Wu, Mineralogical characteristics and oxygen pressure acid leaching of low-grade polymetallic complex chalcopyrite, Journal of Sustainable Metallurgy, 8 (2022), 1628-1638. https://doi.org/10.1007/s40831-022-00594-w

[21] J. A. Sarasua, L. R. Rubio, E. Aranzabe, J. L. V. Vilela, Energetic study of ultrasonic wettability enhancement, Ultrasonics Sonochemistry, 79 (2021) 105768. https://doi.org/10.1016/j.ultsonch.2021.105768

[22] J. Q. Xue, W. B. Mao, X. Lu, J. X. Li, Y. J. Wang, M. Wu, Dynamics of ultrasound-assisted oxidation leaching of nickel sulfide concentrate, Chinese Journal of Nonferrous Metals, 20(5) (2010) 1013-1020. https://doi.org/10.19476/j.ysxb.1004.0609.2010.05.031

[23] G. H. Xia, M. Lu, X. L. Su, X. D. Zhao, Iron removal from kaolin using thiourea assisted by ultrasonic wave, Ultrasonics Sonochemistry, 19(1) (2012) 38-42. https://doi.org/10.1016/j.ultsonch.2011.05.008

[24] J. Q. Xue, X. Lu, Y. W. Du, W. B. Mao, J. X. Li, Y. J. Wang, Ultrasonic-assisted oxidation leaching of nickel sulfide concentrate, Chinese Journal of Chemical Engineering, 18(6) (2010) 948-953.

[25] J. X. Wang, F. Faraji, A. Ghahreman, Effect of ultrasound on the oxidative copper leaching from chalcopyrite in acidic ferric sulfate media, Minerals, 10(7) (2020), 633. https://doi.org/10.3390/min10070633

[26] H. S. Yoon, C. J. Kim, K. W. Chung, J. Y. Lee, S. M. Shin, S. R. Kim, M. H. Jang, J. H. Kim, S. I. Lee, S. J. Yoo. Ultrasonic-assisted leaching kinetics in aqueous $FeCl_3$ -HCl solution for the recovery of copper by hydrometallurgy from poorly soluble chalcopyrite, Korean Journal of Chemical Engineering, 34(6) (2017) 1748-1755. https://doi.org/10.1007/s11814-017-0053-x

[27] J. Rooze, E. V. Rebrov, J. C. Schouten, J. T. F. Keurentjes, Dissolved gas and ultrasonic cavitation - A review, Ultrasonics Sonochemistry, 20(1) (2012) 1-11. https://doi.org/10.1016/j.ultsonch.2012.04.013

[28] Y. M. Wang, A. X. Wu, C. M. Ai. Experiment and mechanism analysis on leaching process of low grade copper sulfide intensified by ultrasonic wave, The Chinese Journal of Nonferrous Metals, 23(7) (2013) 2019-2025. https://doi.org/10.19476/j.ysxb.1004.0609.2013.07.033

[29] Z. Zhang, X. Liu, D. Li, Y. Lei, T. Gao, B. Wu, J. Zhao, Y. Wang, G. Zhou, H. Yao, Mechanism of ultrasonic impregnation on porosity of activated carbons in non-cavitation and cavitation regimes, Ultrasonics Sonochemistry, 51 (2019) 206–213. https://doi.org/10.1016/j.ultsonch.2018.10.024

[30] A. A. Ádám, M. Szabados, G. Varga, Á. Papp, K. Musza, Z. Kónya, Á. Kukovecz, P. Sipos, I. Pálinkó, Ultrasound-assisted hydrazine reduction method for the preparation of nickel nanoparticles, physicochemical characterization and catalytic application in suzuki-miyaura cross-coupling reaction, Nanomaterials 10(2020) 632. https://doi.org/10.3390/nano10040632

[31] Y. L. Yang, Y. F. Shen, J. G. Chen, Y. Wang, Nanocrystalline nickel coating prepared by pulsed electrodeposition combined with ultrasonic agitation, Acta Metallurgica Sinica, 43 (2007) 883–888. https://doi.org/10.1016/j.actamat.2007.05.024

[32] Z. J. Zhang, Analysis on mechanism and influencing factors of ultrasonic assisted extraction, Science and

Technology of Food Industry, 31(4) (2010) 399-401. https://doi.org/10.13386/j.issn1002-0306.2010.04.084

[33] C. F. Dickinson, G. R. Heal. Solid–liquid diffusion controlled rate equations, Thermochimica Acta, 340/341 (1999) 89-103. https://doi.org/10.1016/S0040-6031(99)00256-7

[34] S. Aydogan, Dissolution kinetics of sphalerite with hydrogen peroxide in sulphuric acid medium, Chemical Engineering Journal, 123(3) (2006) 65-70. https://doi.org/10.1016/j.cej.2006.07.001

[35] H. H. Wang, G. Q. Li, D. Zhao, J. H. Ma, J. Yang, Dephosphorization of high phosphorus oolitic hematite by acid leaching and the leaching kinetics, Hydrometallurgy, 171 (2017) 61-68. https://doi.org/10.1016/j.hydromet.2017.04.015

[36] L. Li, Y. Bian, X. Zhang, Y. Guan, E. Fan, F. Wu, R. Chen, Process for recycling mixed-cathode materials from spent lithium-ion batteries and kinetics of leaching, Waste Management, 71 (2018) 362-371. https://doi.org/10.1016/j.wasman.2017.10.028

[37] W. N. Mu, X. Y. Lu, F. H. Cui, S. H. Luo, Y. C. Zhai, Transformation and leaching kinetics of silicon from low-grade nickel laterite ore by pre-roasting and alkaline leaching process, Transactions of Nonferrous Metals Society of China, 28(1) (2018) 169–176. https://doi.org/10.1016/S1003-6326(18)64650-3

[38] L. Xiao, P. W. Han, Y. L. Wang, G. Y. Fu, Z. Sun, S. F. Ye, Silver dissolution in a novel leaching system: Reaction kinetics study, International Journal of Minerals Metallurgy and Materials, 26(2) (2019) 168-177. https://doi.org/10.1007/s12613-019-1721-0

[39] J. Tian, J. Q. Yin, R. Chi, G. Rao, M. Jiang, K. Ouyang, Kinetics on leaching rare earth from the weathered crust elution-deposited rare earth ores with ammonium sulfate solution, Hydrometallurgy, 101(3/4) (2010) 166-170. https://doi.org/10.1016/j.hydromet.2010.01.001